X-ray Emission Signatures of Neutron Star Mergers

Connery J. Chen, Yihan Wang and Bing Zhang

Nevada Center for Astrophysics and University of Nevada, Las Vegas, NV 89154, USA

email: connery.chen@unlv.edu

ABSTRACT

Neutron star (NS) mergers, including both binary NS mergers and black hole-NS mergers, are multimessenger sources detectable in both gravitational waves (GWs) and electromagnetic (EM) radiation. The expected EM emission signatures depend on the source's progenitor, merger remnant, and observer's line of sight (LoS). Widely discussed EM counterparts of NS mergers have been focused in the gamma-ray (in terms of short-duration gamma-ray bursts) and optical (in terms of kilonova) bands. In this paper, we show that X-ray emission carries unique post-merger signatures that are inaccessible in other EM bands and plays an important role in understanding the physics and geometry of NS mergers. We consider several progenitor and central engine models and investigate X-ray emission signatures from the prompt phase immediately after merger to the afterglow phase extending years later. For the prompt phase, we devise a general method for computing phenomenological X-ray light curves and spectra for structured jets viewed from any LoS, which can be applied to prompt X-ray observations of NS mergers to constrain the geometry. The geometric constraints can in turn be used to model the afterglow and estimate a peak time and flux—to preemptively determine afterglow characteristics would be monumental for follow-up observation campaigns of future GW sources. Finally, we provide constraints on the optimal time window for X-ray counterpart searches of NS mergers across a range of luminosity distances and detector sensitivities.

Central Engine

- Black hole (BH) + tidal disruption (TD):
  - Disrupted material forms **accretion disk** which powers jets

$$t_{\rm dyn} = \left(\frac{R^3}{GM}\right)^{1/2} \approx 0.06 \left(\frac{R}{10{\rm km}}\right)^{3/2} \left(\frac{M}{2M_\odot}\right)^{-1/2} \ {\rm ms}$$

- Hypermassive neutron star (HMNS):
  - Supported by **differential rotation**

$$t_A = \frac{R}{v_A} \approx 1 \left(\frac{B_0}{10^{14}\,{\rm G}}\right)^{-1} \left(\frac{R}{10\,{\rm km}}\right)^{-1/2} \left(\frac{M}{2M_\odot}\right)^{1/2} \ {\rm s}$$

- Supramassive neutron star (SMNS):
  - Supported by **rigid rotation**

$$t_c = \frac{a}{2b^2} \ln\left[\left(\frac{a\Omega_0^2 + b}{a\Omega_c^2 + b}\right)\frac{\Omega_c^2}{\Omega_0^2}\right] + \frac{\Omega_0^2 - \Omega_c^2}{2b\Omega_0^2\Omega_c^2} \approx 6.33 \times 10^3 \ {\rm s},$$

where b and a are coefficients of EM and GW losses, respectively

- Stable NS:
  - Radiation powered by **spindown**

$$L_{\rm sd}(t) = \dot{E}_{\rm rot}(t) = I\Omega\dot{\Omega} = -\frac{B_p^2 R^6 \Omega^4(t)}{6c^3} - \frac{32GI\epsilon^2\Omega^6(t)}{5c^5}$$

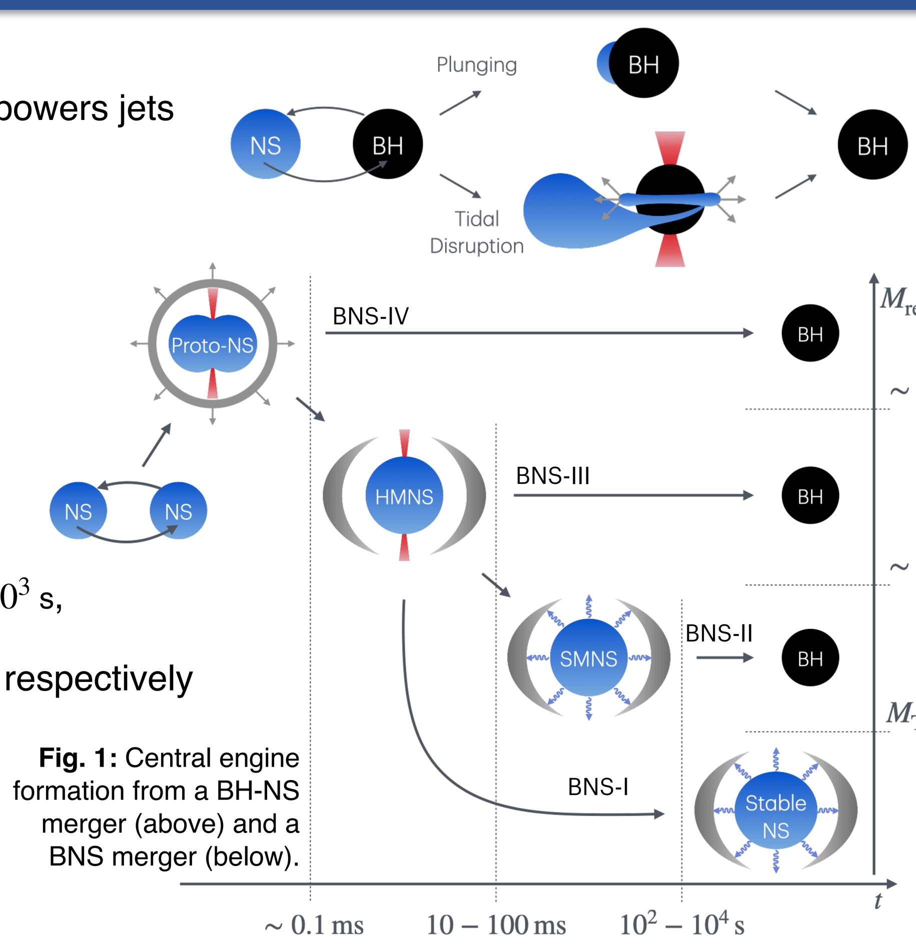

Fig. 1: Central engine formation from a BH-NS merger (above) and a BNS merger (below).

The Doppler factor can generally be written as

$$\mathscr{D} \equiv \frac{1}{\Gamma(1-\beta\cos\theta_v)}$$

On- and off-axis observers each calculate a particular Doppler factor,

$$\mathscr{R}_{\mathscr{D}}(\theta_0,\phi_0,\theta_i,\phi_j) = \frac{\mathscr{D}(\theta_0,\phi_0)}{\mathscr{D}(\theta_i,\phi_j)} = \frac{1-\beta}{1-\beta\cos\theta_w} < 1$$

Relates on- and off-axis observables, e.g.,

$$dt_{\rm off} = \mathscr{R}_{\mathscr{D}}^{-1}\,dt_{\rm on},$$

$$E_{\rm off} = \mathscr{R}_{\mathscr{D}} E_{\rm on},$$

$$\epsilon_{\rm off} = \mathscr{R}_{\mathscr{D}}^{\ 3}\,\epsilon_{\rm on}.$$

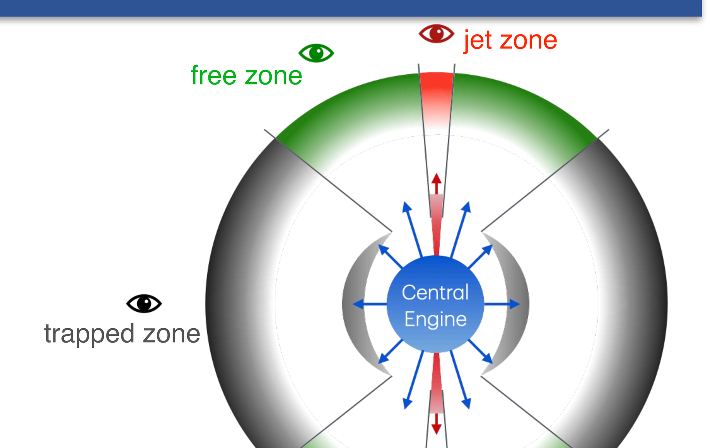

Fig. 2: The geometric configuration of a post-merger central engine.

GW170817 / GRB 170817A

We compile multi-wavelength observations of GRB 170817 and using *VegasAfterglow* perform an MCMC simulation for 30,000 steps:

Table 1: MCMC best-fit parameters.

Model	θ_c [°]	θ_v [°]	$\theta_{\rm cut}$ [°]	$E_{\gamma,{\rm iso}}$ [erg]	Γ_0	$E_{\rm k,iso}$ [erg]	$n_{\rm ism}$ [cm^{-3}]	p	ε_e	ε_B	ξ_n	$E_{\rm inj}$
BNS-I, -II	3	16	20	10^{51}	200	10^{53}	$10^{-2.9}$	2.13	$10^{-2.9}$	$10^{-2.5}$	$10^{-1.2}$	✓
BNS-III, -IV	3	16	20	10^{51}	200	10^{53}	$10^{-2.9}$	2.13	$10^{-2.9}$	$10^{-2.5}$	$10^{-1.2}$	×
BH-NS + TD	10	16	40	10^{50}	200	10^{52}	$10^{-2.9}$	2.13	$10^{-2.9}$	$10^{-2.5}$	$10^{-1.2}$	×

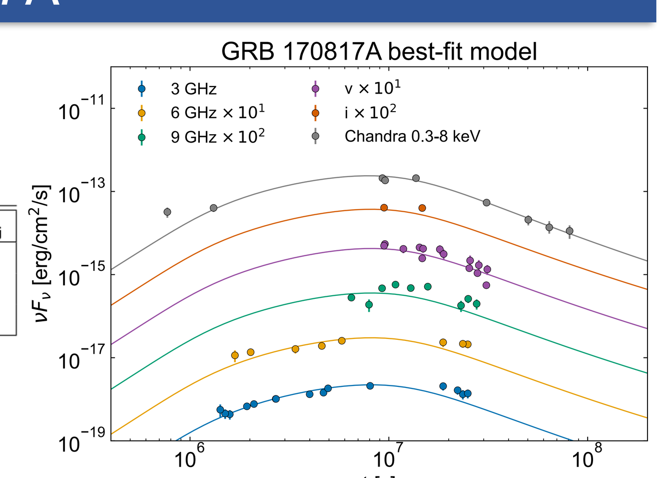

Fig. 5: MCMC best-fit afterglow model for a compiled set of GRB 170817A afterglow data.

We input the best-fit parameters to *PromptX* and successfully reproduce prompt gamma-rays:

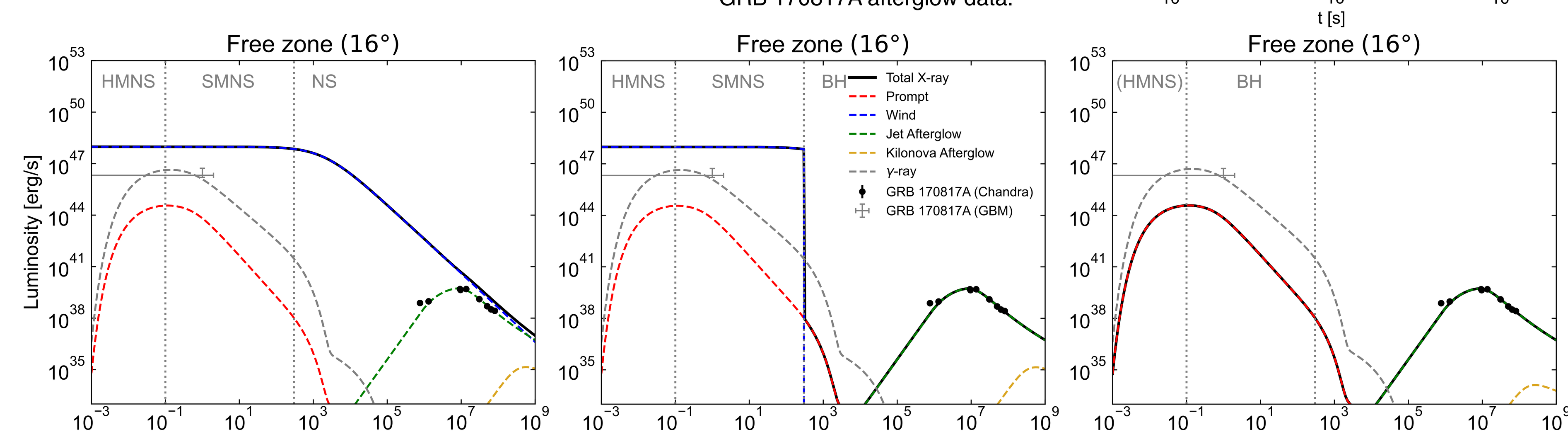

Fig. 6: Model light curves for (clockwise from upper left) BNS-I, BNS-II, BNS-III/BNS-IV, BH-NS using model parameters obtained from MCMC simulations (Table 1). The gray shaded region denotes early times without X-ray coverage.

▸ **BNS-I model ruled out. BNS-II uncertain due to lack of early X-ray coverage. BNS-III/-IV sufficient.**

PromptX

Check it out on GitHub!

Gamma-ray energy profile of the jet:

$$\epsilon_\gamma(\theta) \equiv \frac{dE_\gamma(\theta)}{d\Omega}.$$

The *effective* energy per solid angle is

$$\bar{\epsilon}_\gamma(\theta_0,\phi_0) = k_0 \frac{\sum_{i,j}\epsilon_\gamma(\theta_i,\phi_j)\mathscr{R}_{\mathscr{D}}^3\Delta\Omega_{i,j}}{\sum_{i,j}\Delta\Omega_{i,j}}.$$

Define spectrum, $\mathscr{N}_{i,j}$, and light curve, $\mathscr{L}_{i,j}$, per solid angle.

The total observed spectrum and light curve per solid angle are

$$\mathscr{N}_{\rm tot}(E) = \frac{\sum_{i,j}\mathscr{N}_{i,j}(E)\mathscr{R}_{\mathscr{D}}\Delta\Omega_{i,j}}{\sum_{i,j}\Delta\Omega_{i,j}},$$

$$\mathscr{L}_{\rm tot} = \frac{\sum_{i,j}\mathscr{L}_{i,j}\mathscr{R}_{\mathscr{D}}^4\Delta\Omega_{i,j}}{\sum_{i,j}\Delta\Omega_{i,j}}.$$

The total observed energy per solid angle is

$$\bar{\epsilon} = \int_{E_1}^{E_2} E\mathscr{N}_{\rm tot}(E)\,dE,$$

which gives $E_{\rm iso} = 4\pi\bar{\epsilon}$ in any $E_1 - E_2$ band.

The total observed light curve per solid angle, $\bar{L}$, is obtained by interpolation, which gives $L_{\rm iso} = 4\pi\bar{L}$.

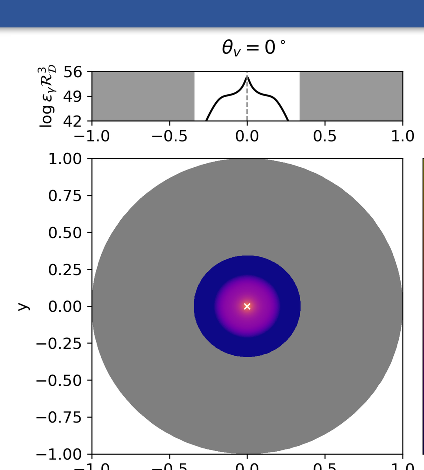

Fig. 3: Maps of observed energy per solid angle for various viewing angles.

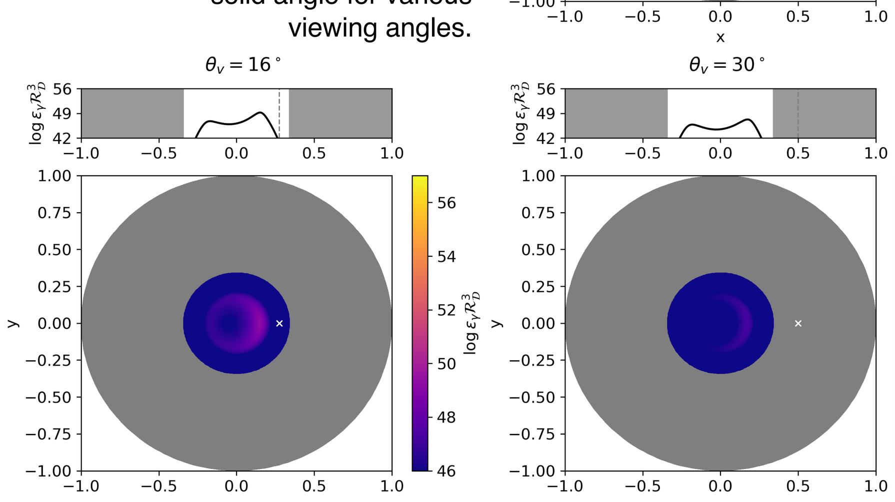

VegasAfterglow

Check it out on GitHub!

Open-source high-performance C++ framework with a user-friendly Python interface for modeling GRB afterglows

- Forward / reverse shock (thin / thick shells)
- Relativistic—non-relativistic regimes
- Adiabatic / radiative blast waves
- Arbitrary structured jet (ϵ,Γ,σ) / medium
- Jet spreading effects
- Arbitrary viewing angles
- Energy injection
- Synchrotron (including self-absorption)
- Inverse Compton with Klein-Nishina corrections

Fig. 4: Convergence and performance test of *VegasAfterglow*—Apple M2 laptop.

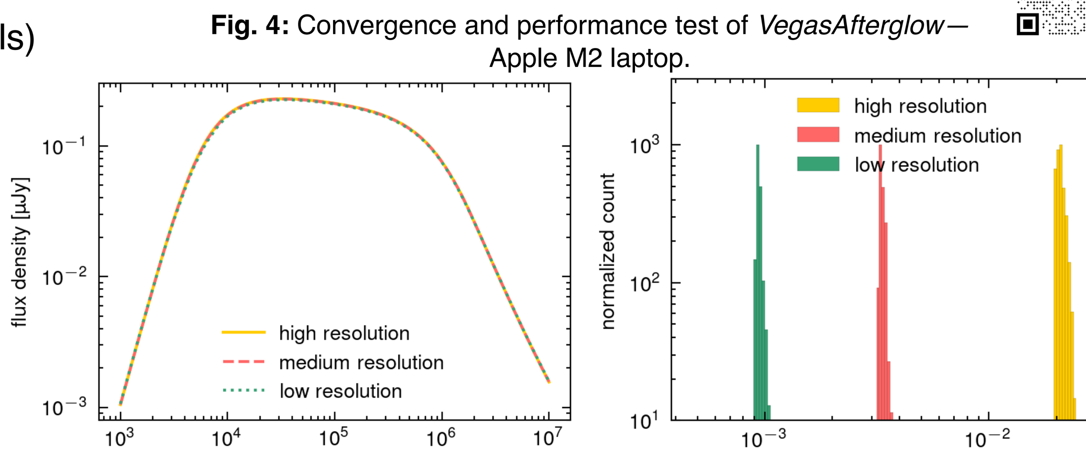

Ongoing Work…Fast X-ray Transients

- A growing number of Fast X-ray Transients (FXTs) have been detected by the Einstein Probe:
  - Energetic extragalactic flashes of X-rays resembling a lower-energy analogue of GRBs.
- Single-component jets:

$$\epsilon_\gamma(\theta) = \begin{cases} \epsilon_{\gamma,0}\exp\left(-\theta^2/\theta_j^2\right), & \theta \le \theta_{\rm cut}, \\ 0, & \theta > \theta_{\rm cut}, \end{cases}$$

where $\epsilon_{\gamma,0}$ is the peak energy per solid angle and θ_j is the Gaussian width, and $\theta_{\rm cut}$ is the cutoff angle.

- Multi-component jet+cocoon:

$$\epsilon(\theta) = \epsilon_{\gamma,0} \times \begin{cases} 1, & 0 \le \theta \le \theta_0, \\ \exp\left[-\frac{1}{2}\left(\frac{\theta-\theta_0}{\theta_j}\right)^2\right], & \theta_0 < \theta \le \theta_j, \\ A_c\left(\frac{\theta}{\theta_j}\right)^{-k_c}, & \theta > \theta_j, \\ 0, & \theta > \theta_{\rm cut}, \end{cases}$$

where θ_0 is the jet core opening angle, θ_j is the jet cocoon Gaussian width, A_c and k_c are the stellar cocoon normalization factor and power-law index, respectively, and $\theta_{\rm cut}$ is the cutoff angle.

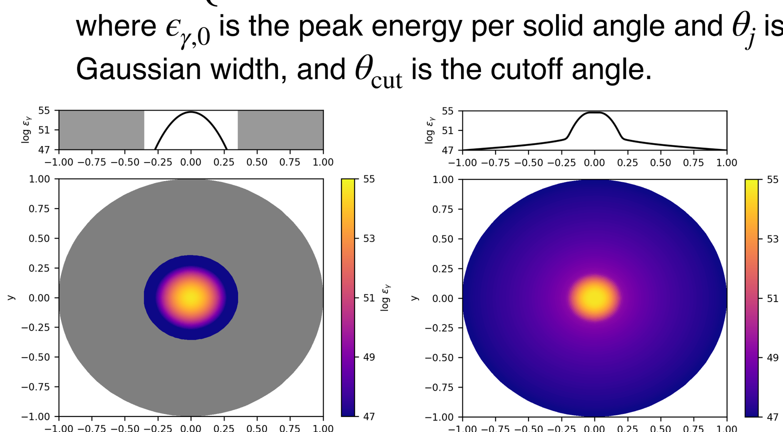

Fig. 10: Intrinsic energy profile of single-component (*left*) and multi-component (*right*) structures.

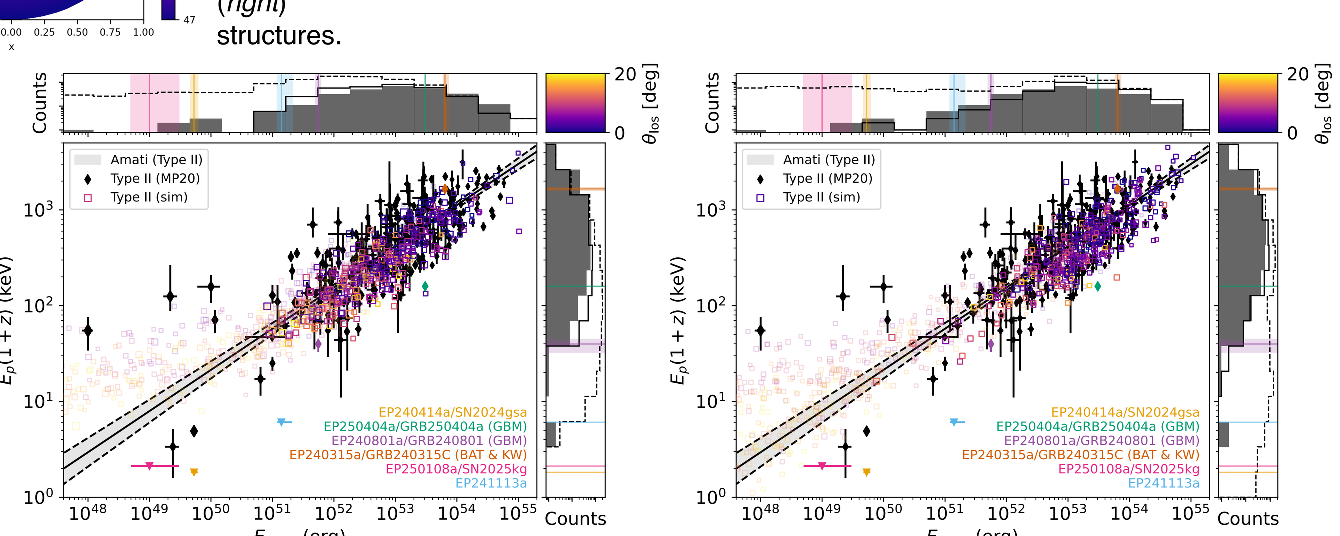

Fig. 11: Simulated (squares) and observed (diamonds) Type II GRBs for a single-component jet (*left*) and multi-component jet+cocoon (*right*). Colors represent θ_v, transparency represents detectability, size represents redshift—lower redshifts appear larger. Plotted in select colors are EP-detected GRBs and FXTs of note. Along the top and right are marginal histograms where dashed (solid) lines show all (detectable) events.

▸ **Preliminary results suggest that FXTs *cannot* be explained under the standard paradigm of Type II GRBs.**

X-ray Counterpart Searches of NS Mergers

- **Detection**: An NS merger event is identified by either a GW signal or Type I GRB
- **Prompt X-ray analysis**: Data from X-ray detectors covering the localization region should be examined for triggers
- **Geometric constraints**: Constraints on θ_c and θ_v for a GW170817-like event from prompt X-rays (Fig. 7)
- **X-ray afterglow predictions**: With geometric constraints, X-ray afterglow characteristics can be estimated (Fig. 8).
- **Coordinated follow-up**: X-ray follow-ups strategized based on predicted afterglow properties. Fig. 9 shows the optimal time window for detecting an X-ray counterpart of an NS merger with known luminosity distance.

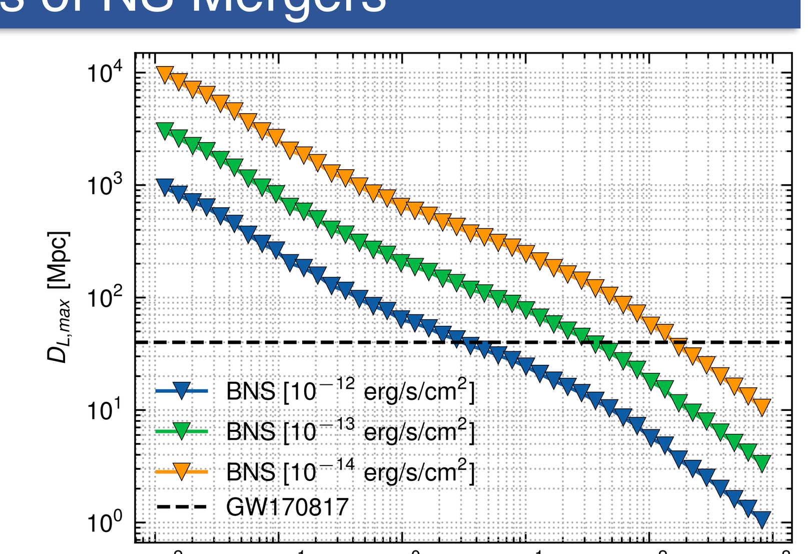

Fig. 9: Detection horizon for X-ray afterglows from BNS mergers.

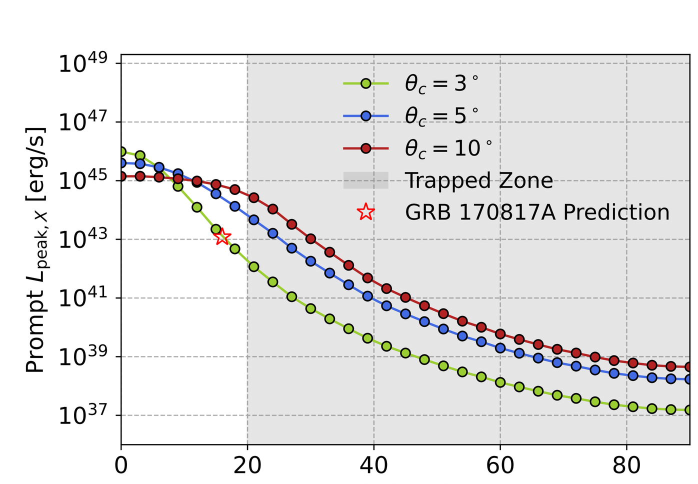

Fig. 7: Prompt X-ray emission peak luminosity as a function of viewing angle.

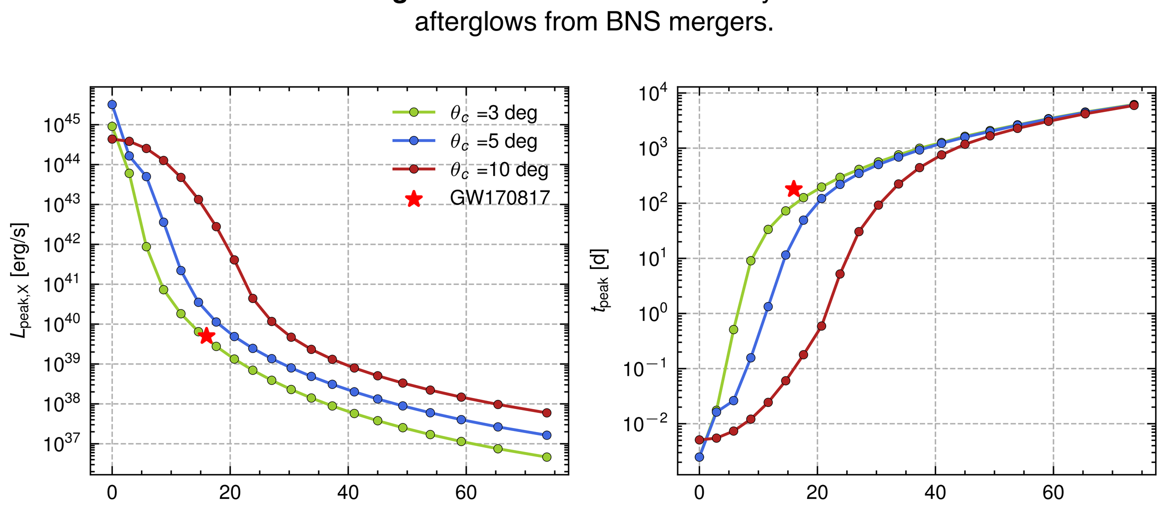

Fig. 8: X-ray afterglow peak luminosity (*left*) and peak time (*right*) as functions of viewing angle for a GW170817-like event.

CONCLUSIONS

- Systematically investigated X-ray signatures from NS mergers for various progenitors and central engines
- Introduced a method to model prompt X-ray light curves/spectra for arbitrary jet profiles
- Highlighted how viewing geometry dramatically influences observed X-ray signatures
- Performed a case study of GRB 170817A using MCMC simulations and showed that the prompt and afterglow frameworks developed here are consistent with observations
- Introduced a basic workflow for identifying and characterizing X-ray counterparts of GW-detected NS mergers, emphasizing rapid and coordinated follow-up strategies

ACKNOWLEDGEMENTS

This work is supported by the University of Nevada, Las Vegas Top-Tier Graduate Research Assistantship, Nevada Center for Astrophysics, and Nevada Space Grant Consortium Graduate Research Fellow Opportunity.

REFERENCES

Chen, C., Wang, Y., & Zhang, B. (2025). *X-ray emission signatures of neutron star mergers* [Preprint]. arXiv. https://doi.org/10.48550/arXiv.2505.01606 [Manuscript submitted for publication]. *The Astrophysical Journal.*

Wang, Y., **Chen, C.**, & Zhang, B. (2026). *VegasAfterglow: A high-performance framework for gamma-ray burst afterglows. Journal of High Energy Astrophysics*, 50, 100490. https://doi.org/10.1016/j.jheap.2025.100490